Resonant tunneling between transverse *X* states in GaAs/AlAs double-barrier structures under elevated hydrostatic pressure

J. M. Smith* and P. C. Klipstein
Clarendon Laboratory, Department of Physics, University of Oxford, Parks Road, Oxford OX1 3PU, United Kingdom

R. Grey and G. Hill
Department of Electrical and Electronic Engineering, University of Sheffield, Mappin Street, Sheffield SI 3JD, United Kingdom
(Received 10 April 1997)

We present a model to describe the mechanisms involved in tunneling between the quasiconfined *X* subbands of the AlAs layers in GaAs/AlAs double-barrier structures at pressures up to the type-II transition. The model involves self-consistent Schrödinger-Poisson calculation of the potential profiles within the device for a given relative alignment between the two *X*-like quantum wells, and thus allows prediction of the bias positions at which certain resonant tunneling processes will occur. By systematic variation of the parameters involved, in particular the charge distribution between the two AlAs layers, these predictions have been fitted to the measured vertical transport characteristics of a series of samples of different AlAs layer width. In the cases of those samples with *X* ground states that are transverse in nature, very good agreement has been obtained. The level of insight afforded by the model opens up alternative methods for the determination of important band-structure parameters, such as the light effective mass of the *X* minima in AlAs, and the Γ_{GaAs}-X_{AlAs} conduction-band offset. It also proves to be an extremely sensitive probe of the degree of symmetry between the AlAs layer widths of near-symmetric devices, and we are thus able to measure an asymmetry of around one monolayer in each of our devices. This explains entirely the asymmetry exhibited by the low bias $X_t(1) \rightarrow X_t(1)$ resonances of some nominally symmetric double-barrier structures, which has been a source of some debate in recent years. [S0163-1829(98)01703-2]

I. INTRODUCTION

The presence of the *X* minima in the AlAs layers of GaAs/AlAs double-barrier structures DBS's is a significant factor in limiting the quality of the measured 1 bar current resonances, relative to that predicted by the simple Γ-point theory,[1–4] and so extensive work has been carried out both in characterizing their static properties, and in determining the extent of their role in the tunneling mechanism. Hydrostatic pressure has been shown to be effective as a means of further accessing the *X* minima, resulting first in the suppression of any Γ-resonance,[5–7] and subsequently in the revelation of numerous resonances that are not apparent at 1 bar.[8–10]

The principal effect of elevated hydrostatic pressure is to reduce the energy of the *X*-like double well profile in the conduction band relative to the Γ-like double-barrier profile, at a rate of around 13 meV kbar^{-1}.[11,12] This enables electrons to transfer from the bulk GaAs contact region into the lowest two-dimensional (2D) quasiconfined state in the adjacent AlAs ''emitter'' layer with the aid of an accumulation region that is progressively smaller with increasing pressure, up to the type-I to type-II transition at P_t ($P_t \sim 9$ kbar for a wide layered DBS). At this pressure no accumulation region is required and the unbiased device becomes an indirect system in both real and reciprocal space.

Many resonances observed at high pressure in DBS's are therefore caused by tunneling between the two sets of quasiconfined states in the *X* wells of the AlAs layers. These states can be separated into transverse $[X_t(n)]$ and longitudinal $[X_l(n)]$ types, corresponding to the *X* minima with large wave vectors perpendicular to, and parallel with, the growth direction (z), respectively. The anisotropy of the minima endows them with two principal effective masses, one of which is in the direction parallel with the large wave vector, and relatively heavy, $m^*_{X,L} = (1.1 \pm 0.2) m_0$, and the other of which is in the plane perpendicular to the large wave vector, and relatively light, $m^*_{X,T} = (0.24 \pm 0.05) m_0$.[13] Competing effects of spatial confinement and compressive strain mean that the ground state in an AlAs layer thicker than ~ 50 Å will be $X_t(1)$, while in a layer narrower than this ''crossover width'' it will be $X_l(1)$.[14] The nature of the ground state is critical in determining both the electrical[15–17] and the optical[14,18] behavior of these devices. In resonant tunneling, the transverse *X* states of a DBS are significantly favored over the longitudinal *X* states, since they possess the lighter mass in the *z* direction and their wave functions therefore suffer less attenuation in the central GaAs layer.[10] The samples studied here have central GaAs layers 40 Å in width, for which the attenuation coefficients of the two *X* orientations are calculated to differ roughly by a factor of $\sim 10^6$. For wide layered DBS's then, in which the first AlAs state to be populated as pressure and bias are applied is $X_t(1)$, it is expected that the tunneling characteristics will be dominated entirely by electrons of a transverse nature.

In this investigation we find that for two DBS's with AlAs layers of 60 Å and of 70 Å in width, all observed resonances can be attributed unambiguously to elastic or inelastic tunneling processes involving only transverse *X* states. This facilitates representation of the band profiles in the device by a simple Schrödinger-Poisson model, from which the applied

bias required for a given resonant process may be calculated. By methodical adjustment of the input parameters it is possible to fit the model very well to the measured data, and as a result, to determine such quantities as the AlAs layer widths and the transverse electron mass quite accurately. Samples with narrower AlAs layers are found to deviate from the simple model, since the mechanism is complicated by the longitudinal nature of the AlAs ground states, but we find that qualitative identification of resonant processes is still possible by comparison with the wider layered samples.

The emitter state for each of the resonant processes discussed here is $X_t(1)$, and the collector states to which tunneling is observed to occur are $X_t(n)$, for $n=1$, 2, and 3. At biases above those of the strong resonances displayed by the elastic processes, weaker features are measured that are attributed to inelastic processes involving the emission of phonons. The phonon energies may also be determined from the model and correspond to the zone centre TO_{GaAs} and TO_{AlAs} modes.

II. EXPERIMENT

The four samples studied were nominally symmetric n-i-n GaAs/AlAs DBS's grown by molecular-beam epitaxy on [100] oriented substrates. They were nominally identical with the exception of the AlAs layer thicknesses, which was varied in 10 Å increments between 40 and 70 Å. This parameter is subsequently named l_w.

The constituent epitaxial layers of a sample with AlAs layers of thickness l_w were as follows: 0.25 μm, $n=1\times10^{18}$ cm^{-3} GaAs:Si buffer, 0.5 μm, $n=2\times10^{17}$ cm^{-3} GaAs:Si, 100 Å undoped (ud) GaAs spacer, l_w Å ud AlAs, 40 Å ud GaAs, l_w Å ud AlAs, 100 Å ud GaAs spacer, 0.5 μm $n=2\times10^{17}$ cm^{-3} GaAs:Si, 0.25 μm $n=1\times10^{18}$ cm^{-3} GaAs:Si cap. Mesa diameters were 20 μm. Layer thicknesses were calibrated using reflection high-energy electron diffraction (RHEED), and the doping concentrations in the layers adjacent to the spacers were additionally measured using a BIO-RAD electrochemical profile plotter. The measured concentrations, which have been used in the calculations, were in all cases less than a factor of 4 different from the nominal values, and are not included here for the sake of clarity.

The two terminal transport measurements were carried out using a combined voltage source and virtual ground current amplifier system. Conductance measurements were made by modulating the applied voltage with a sinusoid of 1 mV rms, and $\sim$1 kHz, and subsequently detecting the ac signal with a lock-in amplifier. Hydrostatic pressure was applied using a clamp cell, equipped with an *in situ* manganin wire manometer.

A set of I-V and conductance (I'-V) measurements were made on each of the four samples, at regular pressure intervals from 1 bar up to 1 or 2 kbars above the signature of the type I to type II transition, and, at each of these pressures, at three or four temperatures between 100 and 4.2 K.

III. MODELING

The simplest form of the model, as described here, is based on the existence solely of transverse X states in the AlAs layers, and is therefore suitable for modeling only wide layered DBS's. The modeling of narrow layered DBS's is somewhat more involved since tunneling from both longitudinal and transverse states may contribute to the vertical transport characteristics. Adaptations to incorporate longitudinal intravalley processes, or even intervalley processes involving both longitudinal and transverse states, should be possible, but have yet to be tested against experimental measurements.

At low temperature, the Fermi energy in the n-type contact regions is pinned very close to the donor energy, which is around 6 meV below the conduction-band edge of the bulk GaAs. This pinning is a result of the background acceptor states that occur in GaAs being filled, and so ensuring that the donor level is partially empty. The key assumption of the model is that for a given pressure $P<P_t$, the application of bias aligns the contact Fermi energy with the $X_t(1)$ state in the emitter AlAs layer for a size of accumulation layer that is dictated by the interface band alignment between the Γ minimum in GaAs and the $X_t(1)$ state. This energy separation is in turn equal to the sum of the interface band offset Γ_{GaAs}-$X_{t,AlAs}$, and the confinement energy of $X_t(1)$ within the X well. The Γ_{GaAs}-$X_{t,AlAs}$ band offset is written as $\Delta_{\Gamma\text{-}X}$ and is a function of pressure given by

$$\Delta_{\Gamma\text{-}X}(P)\approx\Delta^0_{\Gamma\text{-}X}-13P-8, \tag{1}$$

where units used are meV and kbars. The value of the pressure coefficient has been taken from Skolnick *et al.*[11] and the -8 meV term accounts for the effect of the compressive strain on the transverse minima relative to their energy in a relaxed crystal. [For longitudinal minima this is substituted with $+16$ meV, the difference between the two thus equaling the accepted strain splitting of $\sim$24 meV (Ref. 14)] $\Delta^0_{\Gamma\text{-}X}$ is a quantity for which estimates have varied. From the measurements of P_1 made in this investigation, a value of $\Delta^0_{\Gamma\text{-}X}=(114\pm10)$ meV is indicated. For a known offset energy, the accumulation region is solved uniquely using a self-consistent Schrödinger-Poisson model. The onset of vertical current flow is expected to occur only when charge first transfers into the $X_t(1)$ state as the bias is further increased from this threshold value.

We assume that the thermal equilibrium distribution of electrons in the emitter contact and accumulation regions extends into the emitter AlAs layer. This is true as long as Γ-X_t transfer across the emitter interface is a faster process than tunneling through the central GaAs layer, for which there exists good supporting evidence.[19] The density of states (DOS) of the $X_t(1)$ subband is given by

$$\frac{\partial n}{\partial E}=4\frac{m^*_{geo}}{\hbar^2\pi}, \tag{2}$$

where m^*_{geo} [$=\sqrt{m^*_{X,T}m^*_{X,L}}\approx0.5m_0$] is the geometric average effective mass of the X minima in the plane of the layers, and the factor of four accounts for the four degenerate transverse X minima in the first Brillouin zone. The result is a DOS of around 10^{12} cm^{-2} meV^{-1}, some thirty times larger than that of the Γ minimum in GaAs.

The electric field (ξ_0) at the GaAs spacer/AlAs emitter layer interface is uniquely determined by the accumulation

layer solution. As bias is further increased, charge transfers from the contact region into the $X_t(1)$ subband, causing further Coulomb band bending and therefore greater electric field in the remaining ud region. The high DOS of $X_t(1)$ ensures that, under the experimental conditions employed here ($P<P_t$, $|V_{\text{bias}}|<2$ V), the Fermi energy never rises more than 1 meV above the subband minimum. The accumulation region for all observed resonances can thus be considered, for a particular device, as a function of pressure only.

Self-consistent solution of the double well X profile is therefore achieved by fixing ξ_0, corresponding to a known accumulation layer, and finding the additional charge density required in the emitter $X_t(1)$ state to align it with the desired state energy, or ''state+phonon'' energy, in the collector well. At the same time, a fraction of this charge density—the reciprocal of which we define as the parameter r—is included in the collector AlAs layer. The parameter r is thought to be approximately constant for a specified resonant process, sample, and temperature, by the following argument: At dynamic equilibrium,

$$\frac{\partial n_{\text{coll}}}{\partial t} \approx \frac{n_{\text{emit}}}{\tau_{\text{emit}}} - \frac{n_{\text{coll}}}{\tau_{\text{coll}}} = 0, \tag{3}$$

where the emitter and collector wells are indicated by the subscripts, and n and τ represent the associated electron densities and the times taken for electrons to escape through the collector ''barrier'' of the well concerned. τ_{emit} is principally governed by the strength of the matrix element for the particular resonant process, and τ_{coll} by the X-Γ matrix element at the collector well/spacer interface, both of which are thought to be independent of pressure, so

$$\frac{n_{\text{emit}}}{n_{\text{coll}}} = \frac{\tau_{\text{emit}}}{\tau_{\text{coll}}} = r \approx \text{const.} \tag{4}$$

The calculations themselves utilize simple one band transfer matrices to model wave function propagation through a potential profile, which is divided into 1 Å-thick slices of uniform potential. Quasiconfined states in the two wells are located independently using exponential boundary conditions at selected points in the barrier regions, and the charge distribution throughout the structure is calculated from their normalized wave functions and total charge densities. Γ and X potential profiles and wave functions for a typical $X_t(1)\rightarrow X_t(2)$ resonance are shown in Fig. 1. A parameter u is defined, which represents the energy difference between the two $X_t(1)$ states under bias and therefore has a unique value for each resonance observed.

The confinement energy of the confined Γ state in the central GaAs layer is around 150 meV. This is sufficient to place it above the resonant energy, and therefore without influence on the X-like process, for applied biases less than about 1 V. Higher biases than this may involve the transfer of electrons from the emitter $X_t(1)$ state into this Γ state, further complicating the distribution of charge throughout the device.

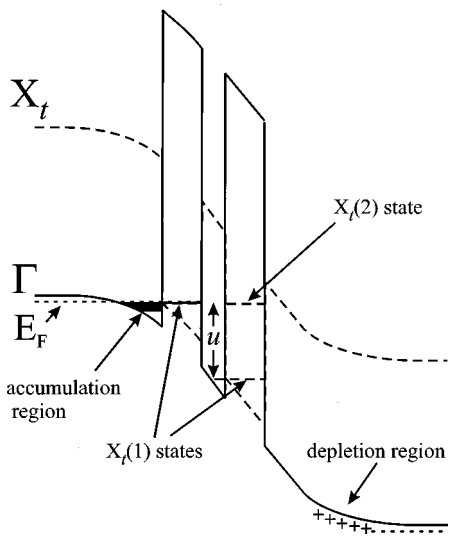

FIG. 1. Band profile diagram for the Γ and X_t minima of a DBS under bias and with $P<P_t$ and $T=4.2$ K. The $X_t(1)\rightarrow X_t(2)$ resonant process is energetically aligned, and the energy difference u between the ground states of the two AlAs layers is defined.

IV. RESULTS AND ANALYSIS

Measured resonances due to elastic tunneling processes are displayed in Fig. 2. Four current-voltage I-V plots show the process $X_t(1)\rightarrow X_t(2)$ for each of the samples, and additionally $X_t(1)\rightarrow X_t(3)$ for the two wider layered samples. The general trend of resonance bias positions is to the reduction of bias with increased well width, consistent with a reduced u value for a given elastic process.

Figure 3 shows the conductance curve measured from the 70 Å sample at 4.2 K and 9 kbar. It is typical of the four

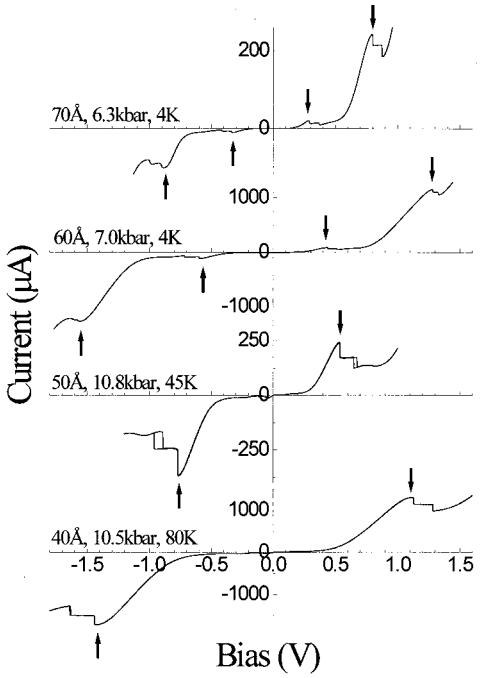

FIG. 2. $I-V$ characteristics of the four samples measured. The resonances due to elastic tunneling processes are marked. Note the higher temperature needed to excite electrons into the $X_t(1)$ emitter state for the two narrower layered samples.

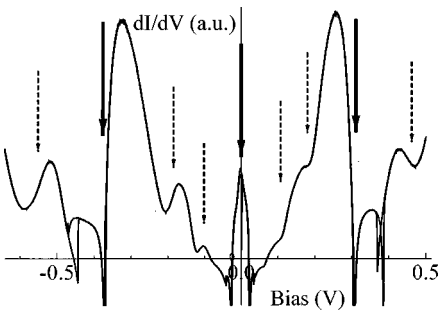

FIG. 3. Conductance data from the 70 Å sample at 9 kbar and 4.2 K. The bold, solid arrows indicate elastic processes while the dotted arrows indicate their phonon satellites.

samples in its general form, with large, hysteretic negative conductance regions caused by the $X_t(1)\rightarrow X_t(2)$ resonances, and a strong $X_t(1)\rightarrow X_t(1)$ peak near to zero bias indicating that, in this case, $P>P_t$. Three weaker features are seen in each bias direction—two above $X_t(1)\rightarrow X_t(1)$ in bias, and one above $X_t(1)\rightarrow X_t(2)$. They are attributed to zone-center optical-phonon satellites of the elastic processes, and will be discussed further in due course.

The analysis of these resonances is based, as was indicated in the previous section, on the modeling of the pressure dependence of their bias positions. Figure 4 shows the best fits achieved for the 70 and 60 Å samples for all of the resonances in Fig. 3, with the exception of $X_t(1)\rightarrow X_t(1)$, at pressures reaching up to around 1 kbar past P_t [the signature of the type I to type II transition being the onset of $X_t(1)\rightarrow X_t(1)$]. We identify the position of each phonon resonance in Fig. 4 by the point of inflection following each conductance peak. Both bias directions are shown as positive so that more direct comparison between them may be made. The $X_t(1)\rightarrow X_t(3)$ resonances are not shown, since the

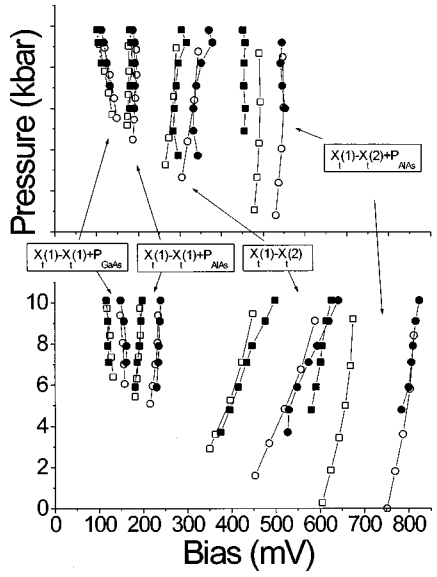

FIG. 4. Best fits to the bias position pressure dependences up to the type II transition, of the samples with 70 Å (upper plot) and 60 Å AlAs layer widths, using the Schrodinger-Poisson model. Open symbols correspond to theory, closed symbols to experiment, squares to forward bias, and circles to reverse. Each resonance is identified on the plot. The fitted parameters are given in Table I.

TABLE I. Parameters used for the theoretical curves of Fig. 4. m_1^* is for $X_t(1)$ and m_2^* for $X_t(2)$ resonances. $r_1,\ldots,r_4$ correspond to the ratio of charge densities in the emitter and collector AlAs layers for the four resonant processes in order of ascending bias.

Sample Parameter	60-40-56	70-40-67
$m(1)^*/m_0$	0.24	0.24
$m(2)^*/m_0$	0.25	0.25
r_1	2	5
r_2	1.4	1.5
r_3	1.2	1.5
r_4	2.5	3
P_{GaAs} (meV)	32	33
P_{AlAs} (meV)	43	42

$X_t(3)$ confined states lie near the top of the X wells and are more difficult to model accurately under the high biases involved. The parameters used to achieve the fitting in Fig. 4 are listed in Table I. The procedure used to fix their values is discussed below.

The first step in the fitting procedure is to adjust the pressure scale. Using Eq. (1) along with the measurements of P_t for the four samples indicates that $\Delta^0_{\Gamma-x}$ is somewhat lower than many previous estimates, at around 114 meV, with a tolerance of ± 10 meV estimated from the spread of P_t values and the tolerance on the pressure coefficient. This figure is consistent with a conduction-band/valence-band offset ratio of 63:37 for the GaAs/AlAs interface.

Next to be dealt with is the asymmetry between the forward and reverse bias directions. It is clear from Fig. 4 that the reverse bias (substrate negatively biased) resonances in both samples appear at consistently higher bias than do their forward bias counterparts. That this is due to differences between the contact doping concentrations has been ruled out from the BIO-RAD measurements, and the only other feasible explanation is that differences exist between the AlAs layer widths. Since RHEED calibration of the layers is most reliable at the start of their growth, when the epitaxial rate corresponds to that which gives strong oscillations during calibration, we take the value of l_w for the AlAs layer located nearer the substrate to be accurate in each case. By decreasing the width of the other layer in the model, the differences between the bias directions for the set of resonances may be fitted. The remaining parameters that have not yet been fitted, in particular the confinement effective mass, may be approximated to their nominal values for this step since they do not contribute directly to the asymmetry. Fitted ''upper AlAs layer'' widths for the 70 and 60 Å samples are 67 and 56 Å, respectively, providing good agreement in each case for at least three of the four resonances. The two samples with narrower AlAs layers also revealed asymmetries of around one monolayer, and in the same sense. The tolerance on the fits is of order ± 1 Å.

For some time the source of asymmetry in the I-V characteristics of the $X_t(1)\rightarrow X_t(1)$ resonance in nominally symmetric DBS's like these has been debated. Figure 5 shows conductance and I-V curves at $P>P_t$ for this resonance in the 70 and 40 Å samples, which are typical of those measured previously. They both are modeled as having asym-

metric layer widths, and yet the 70 Å sample shows no asymmetry in its tunneling characteristics. The explanation for this lies in the pinning of the Fermi energy to the ground X states in the type II pressure regime. If the ground states are $X_t(1)$, as in the 70 Å sample, then they are pinned together at zero bias despite the layer width asymmetry, and the resonant peak must remain at the origin. If, however, $X_l(1)$ are the ground states, then instead they are pinned together, and the lighter $X_t(1)$ states remain misaligned so that the conductance peak occurs in reverse bias. Under conditions in which no zero-bias pinning occurs, the bias positions of the $X_t(1)\rightarrow X_t(1)$ conductance peaks in all four samples occur under small reverse biases that are in good agreement with those predicted by the model for these layer widths.

Asymmetry in the I-V characteristics of $X_t(1)\rightarrow X_t(1)$ for narrow layered samples is directly dependent on the width of the conductance peak—a narrower conductance peak integrating over bias to give a greater asymmetry for a given peak bias position. This width is likely to be closely linked to the layer uniformity, which affects the energy widths of the participating quasiconfined states, and to the interface quality, which determines the distribution of in-plane wave vectors that interface scattering imparts to the tunneling electrons, and thus the range of misalignments between the participating states for which the tunneling process may occur. The peak current asymmetries of up to 6:1 measured by Austing *et al.*[15] may thus in part reflect simply a high quality of heterostructure. Contrary to previous assignment by us,[20] there is no evidence, in the light of these new findings, that differences between the normal (AlAs on GaAs) and inverted (GaAs on AlAs) interfaces play a significant role in any of these measured asymmetries.

The absolute bias positions of the $X_t(1)\rightarrow X_t(2)$ resonances are clearly strongly dependent on the confinement energies of the transverse X states, and thus on the light effective mass $m^*_{X,T}$. Best fits to the data yield $m^*_{X,T}=(0.25\pm 0.03)m_0$, where around 50% of the tolerance derives from a factor of 2 tolerance bestowed on the measured contact doping concentrations.

Fitting the inelastic processes is a simple matter of misaligning the emitter and collector states of the elastic ''parent'' resonance by a fixed energy equal to that of the phonon. The resonant process is thus written $X_t(1)\rightarrow X_t(n)+P$, indicating emission of a phonon P. For the two distinct features directly above the $X_t(1)\rightarrow X_t(1)$ resonance of the 70 Å sample, the energies fitted were (33 ± 1) meV and (42 ± 2) meV, and in the case of the 60 Å sample they were (32 ± 1) meV and (43 ± 2) meV. The features observed above the $X_t(1)\rightarrow X_t(2)$ resonances are also fitted reasonably well by the larger of these two energies in each sample. The errors represent the ranges of energies over which the experimental and theoretical curves in Fig. 4 coincide reasonably well.

It is certain that these inelastic processes are intravalley, and thus involve Γ-point phonons, since no resonances are observed that involve longitudinal collector states and so must be much weaker. Previous publications have focused on scattering by LO phonons, of energies 36 meV and 49 meV in GaAs and AlAs, respectively, because this is usually dominant due to the large Fröhlich coupling in bulk materials. The energies fitted above, however, agree much more closely with those of TO phonons, their being 33 meV (Ref. 13) and 45 meV (Ref. 21) in the two respective materials. We thus assign the collector states of the inelastic processes to $X_t(1)+\mathrm{TO}_{\mathrm{GaAs}}$, $X_t(1)+\mathrm{TO}_{\mathrm{AlAs}}$, and $X_t(2)+\mathrm{TO}_{\mathrm{AlAs}}$. It is perhaps due to the confinement of the phonons into 2D layers that the dominance of electron—LO phonon coupling should be suppressed here, allowing TO mode emission to dominate.

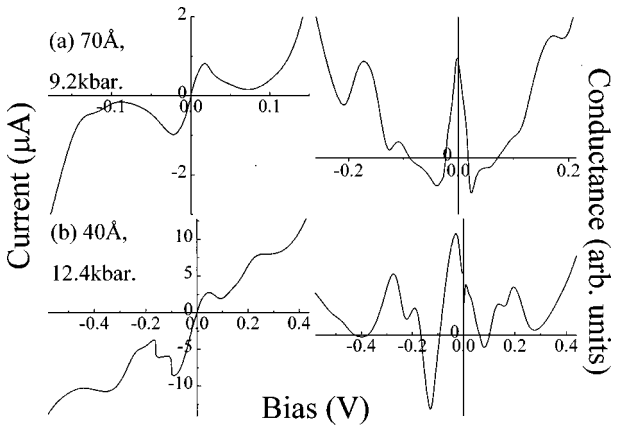

FIG. 5. $I-V$ and conductance characteristics at 4.2 K for low bias and with $P>P_t$ for (a) the 70 Å sample, which displays an I-V characteristic and an $X_t(1)\rightarrow X_t(1)$ conductance peak that are symmetric at zero bias, and (b) the 40 Å sample, with an asymmetric $X_t(1)\rightarrow X_t(1)$ I-V caused by the reverse bias positioning of its conductance peak.

Finally, the fitted values for the ratio r between the charge densities in the emitter and collector wells ($1\leqslant r\leqslant\infty$) should be discussed. These are given in Table I. As r is decreased, the bias position of a particular resonance at a given pressure increases, since the effect is to increase the space charge occupying the collector AlAs layer. For higher pressures, and thus lower ξ_0, the greater charge density required in the emitter AlAs layer to align the resonance means that a given value of r places a higher absolute charge density in the collector well than it does at a lower pressure, and so increases the bias position to a greater extent. In this way, as r is varied the model produces a *fanlike* set of curves for bias vs pressure, all of which intersect at the threshold pressure of the particular resonance. Figure 4 shows that the data for each resonance may be fitted reasonably well for a particular value of r. Note in Fig. 4 that the inelastic processes have r values that are in general higher than the elastic processes. By comparison with Eq. (4) this is consistent with longer emitter state lifetimes, as one would expect with the additional phonon involvement.

The samples with AlAs layers thinner than 60 Å, and so with $X_l(1)$ ground states, display temperature activation of their transverse resonances, since electrons must generally be thermally excited into the $X_t(1)$ emitter state before they can tunnel. For the sample with 50 Å AlAs layers the $X_t(1)$ and $X_l(1)$ levels are almost degenerate so that it is still possible to obtain good fits to the bias positions of the $X_t(1)\rightarrow X_t(2)$ process and its phonon satellite, which may still be observed at 4.2 K. However, to guarantee the purely transverse nature of both the lower bias resonances of this sample, and of all resonances exhibited by the 40 Å sample, higher tempera-

tures must be used. The consequential spreading of the Fermi-Dirac electron distribution together with the fact that the density of states of the $X_l(1)$ emitter ground level is around a factor of 4 lower than for $X_t(1)$, means that the pinning effect between the contact and the emitter state becomes much weaker. The model is thus less suitable for application to these resonances. In practice, we find that the same quality of fits as for the wide layered samples is indeed not possible, and the role of the model is therefore reduced to a qualitative one. Mention should be made however of the fact that at 4.2 K clear resonant features may be observed in the characteristics of these samples (e.g., in Fig. 5 for the 40 Å sample). Although these resonances look similar to those for the wide layered samples, detailed temperature dependence data reveals them to be of different origin, becoming visible only after the temperature activated process have been suppressed. They are therefore believed to result from tunneling between X_t states, but with additional involvement of the emitter $X_l(1)$ state. Further details will be discussed in a future publication.

V. SUMMARY

We have measured the vertical transport characteristics of four GaAs/AlAs DBS's at pressures up to their type-I to type-II transitions and at 4.2 K. They exhibit resonances that have been unambiguously identified as originating from 2D-2D tunneling processes with $X_t(1)$ emitter states and the collector states $X_t(1)$, $X_t(1)+\mathrm{TO}_{\mathrm{GaAs}}$, $X_t(1)+\mathrm{TO}_{\mathrm{AlAs}}$, $X_t(2)$, $X_t(2)+\mathrm{TO}_{\mathrm{AlAs}}$, and $X_t(3)$. The key to these attributions is the Schrödinger-Poisson modeling of the pressure dependences of resonant bias positions in the two samples with $X_t(1)$ ground states in their AlAs layers. The modeling further reveals a degree of asymmetry in the AlAs layer thickness of our samples, of around one monolayer, highlighting the sensitivity of these measurements to such parameters, and providing conclusive explanation for the asymmetry in the I-V characteristics of the $X_t(1)\rightarrow X_t(1)$ resonances displayed by similar samples, that have been the source of some debate. Fitting of the model to the measured $X_t(1)\rightarrow X_t(2)$ resonance has produced a value for the light effective X mass of $m^*_{X,T}=(0.25\pm 0.03)m_0$.

ACKNOWLEDGMENTS

This work was funded by the Engineering and Physical Sciences Research Council (EPSRC), and J.M.S. acknowledges additional support from the General Electric Company (GEC). We also thank Professor M. E. Eremets for his work in the design and construction of the pressure cell.

*Present address: Research Dept. (0500), Electronics and Telecommunications Research Institute (ETRI), 161 Kajong-dong-Gu, Taejon 305-350, S. Korea.

[1] I. Hase, H. Kawai, K. Kaneko, and N. Watanabe, J. Appl. Phys. **59**, 3792 (1986).

[2] E. E. Mendez, E. Calleja, C. E. T. Gonçalves da Silva, L. L. Chang, and W. I. Wang, Phys. Rev. B **33**, 7368 (1986).

[3] P. M. Solomon, S. L. Wright, and C. Lanza, Superlattices Microstruct. **2**, 521 (1986).

[4] A. R. Bonnefoi, T. C. McGill, R. D. Burnham, and G. B. Anderson, Appl. Phys. Lett. **50**, 344 (1987).

[5] E. E. Mendez and E. Calleja, Appl. Phys. Lett. **53**, 977 (1988).

[6] R. Pritchard, P. C. Klipstein, N. R. Couch, T. M. Kerr, J. S. Roberts, P. Mistry, B. Soylu, and W. M. Stobbs, Semicond. Sci. Technol. **4**, 754 (1989).

[7] T. J. Foster, M. L. Leadbeater, D. K. Maude, E. S. Alves, L. Eaves, M. Henini, O. H. Hughes, A. Celeste, J. C. Portal, D. Lancefield, and R. A. Adams, Solid-State Electron. **32**, 1731 (1989).

[8] D. G. Austing, P. C. Klipstein, J. S. Roberts, and G. Hill, Solid State Commun. **75**, 697 (1990).

[9] E. E. Mendez and L. L. Chang, Surf. Sci. **229**, 173 (1990).

[10] D. G. Austing, P. C. Klipstein, A. W. Higgs, H. J. Hutchinson, G. W. Smith, J. S. Roberts, and G. Hill, Phys. Rev. B **47**, 1419 (1993).

[11] M. S. Skolnick, G. W. Smith, I. L. Spain, C. R. Whitehouse, D. C. Herbert, D. M. Whittaker, and L. J. Reed, Phys. Rev. B **39**, 11 191 (1989).

[12] Using values for the pressure dependences of the bulk GaAs direct gap ($+10.7$ meV kbar^{-1}) and of the bulk AlAs indirect gap (-1.5 meV kbar^{-1}), and by adopting a shift into the valence band of the Γ-point band offset ratio between the materials of 0.1% kbar^{-1}. From Adachi (Ref. 13).

[13] S. Adachi, *GaAs and Related Materials, Bulk Semiconducting and Superlattice Properties* (World Scientific, Singapore, 1994).

[14] P. Dawson, C. T. Foxon, and H. W. van Kesteren Semicond. Sci. Technol. **5**, 54 (1990).

[15] D. G. Austing, P. C. Klipstein, J. S. Roberts, C. B. Button, and G. Hill, Phys. Rev. B **48**, 11 905 (1993).

[16] A. F. W. van der Stadt, P. M. Koenraad, J. A. A. J. Perenboom, and J. H. Wolter, Surf. Sci. **362**, 521 (1996).

[17] S. Yamada, K. Maezawa, W. T. Yuen, and R. A. Stradling, Phys. Rev. B **49**, 2189 (1994).

[18] W. R. Tribe, P. C. Klipstein, R. Grey, J. S. Roberts, and G. W. Smith, J. Phys. Chem. Solids **56**, 429 (1995).

[19] The tunneling of X_t electrons through a 40 Å GaAs layer has a similar transmission probability to that of Γ electrons tunneling through a 30 Å AlAs layer. It is well known that the dominance of intervalley transfer over Γ-like tunneling through the emitter barrier region is responsible for the rapid suppression with pressure of the Γ resonance in narrow layered (e.g., 30-40-30) DBS's.

[20] J. M. Smith, D. G. Austing, R. Grey, J. S. Roberts, G. Hill, and P. C. Klipstein, J. Phys. Chem. Solids **56**, 475 (1995).

[21] W. R. Tribe, P. C. Klipstein, G. W. Smith, and R. Grey, Phys. Rev. B **54**, 8721 (1996).